ELSEVIER

Journal of Alloys and Compounds 303–304 (2000) 472–479

Journal of ALLOYS AND COMPOUNDS

www.elsevier.com/locate/jallcom

Resonant X-ray magnetic scattering: antiferromagnetic metals

N. Bernhoeft*

CEA/Grenoble, DRFMC-LCP, 38054 Grenoble, France

Abstract

Resonant X-ray magnetic scattering is a recognized tool for the investigation of new magnetic phases and phase transitions. Many experiments on antiferromagnetic materials involve excitation to valence (band) states for which the density of levels extends over a large interval in comparison with Γ, where Γ/h is the inverse core hole lifetime. A simple model, for the analysis of resonant magnetic scattering from antiferromagnetic materials, is put forward in two stages. First, the antiferromagnetic narrow-band limit is treated and the suggested framework illustrated with an elementary, parametric, analysis of the anomalous resonant energy line shapes observed at the Dy $L_{2,3}$ edges in the intermetallic compound $DyFe_4Al_8$. The method is then extended to deal with intermediate levels which have a bandwidth significant on the scale of Γ.

Keywords: Resonant X-ray magnetic scattering; Narrow band; Antiferromagnetic materials; L edges

1. Introduction

The coupling of photon (electric) and electron (charge) fields has long been exploited in X-ray diffraction techniques. Recently, stimulated by the availability of intense, tunable, X-ray sources provided by new generation synchrotron radiation facilities, considerable experimental and theoretical interest has focused on the phenomenon of resonant (electric multipole) scattering of X-rays which occurs in the vicinity of an absorption edge [1]. The characteristic energy of the resonant scattering/absorption process yields element-specific information which has found application in many fields of research including the biological and material, as well as the chemical and physical sciences. In particular, it proves possible to use the resonant scattering of X-rays as a probe of magnetic phenomena in solids [2]. The unique combination of element and magnetic polarisation sensitivity has opened up new fields of inquiry. The technique as developed to date, relies upon the resonant enhancement of the electric multipole transitions, the weaker magnetic multipole transitions generally being neglected.

At the individual ion level, the resonant elastic matrix element represents the (virtual) excitation of a core level electron to an unoccupied level and the subsequent emission of an outgoing photon with repopulation of the initial electronic state. In the following we present the derivation of a primitive 'hybrid' cross-section specifically aimed at the antiferromagnetic state. The model is hybrid in the sense that the core states are taken as localised whilst the intermediate levels are treated as extended states. The procedure is to be distinguished from more formal methods [3]. The paper is laid out as follows: first, we consider the influence of the antiferromagnetic potential, g, on narrow energy bands. This covers bands (much) less than Γ in width, where Γ/h is the inverse core hole lifetime. At this point there are two energy scales of importance, Γ and g; the effective band width, W, not explicitly appearing. The antiferromagnetic polarisation, ε, may be considered as a functional of g; however, in this work no attempt has been made to link ε and g in a self consistent manner. Having discussed limiting forms of the cross-section (Section 2.2) the formalism developed is used, Section 2.3, as a basis for a phenomenological interpretation of the asymmetric and non-Lorentzian dependence of the cross-section on the incident photon energy at the rare earth L_2 and L_3 edges in the intermetallic compound $DyFe_4Al_8$ [4]. In Sections 3.1–3.4 the arguments are extended to bands of width, W, significant on the scale of Γ. For simplicity, in both Sections 2 and 3, the different orbital projections, m_l, of a given sub-band are taken to have uniform occupation probability (i.e. zero orbital angular momentum) and their spin–orbit splitting, ζ_{so}, is ignored. Both effects may be

*Fax: +33-4-7688-5096.

E-mail address: bern@drfmc.ceng.cea.fr (N. Bernhoeft)

0925-8388/00/$ – see front matter
PII: S0925-8388(00)00629-0

added by simple extension of the given ideas. Finally in Section 4, we summarise our findings and indicate some possible future directions.

2. Experimental

2.1. Antiferromagnetic polarisation of narrow bands

There are two points to be introduced: first, the antiferromagnetic state involves a spatial redistribution of 'up' and 'down' spin electron (quasiparticle) density on two magnetic sublattices and second, the wide (on the scale of Γ) distribution of available intermediate levels in the resonant scattering process. To simplify the discussion, and since it is a useful working limit, we consider initially the narrow-band antiferromagnetic state, $W \ll \Gamma$.

As indicated, the proposed scheme has, unlike the isolated ion model, no energy splitting of spin states; rather, there is a preferential spatial redistribution of the 'up' and 'down' spin electron (quasiparticle) density on two magnetic sublattices. This spatial redistribution sustains, in a self-consistent manner, a modified lattice potential responsible for doubling the unit cell below T_N and separating the spin 'up' and spin 'down' states in momentum space. The lattice potential, which splits a given paramagnetic band into two on doubling the unit cell, is characterised by the parameter g. The lower and upper bands are labeled as 1 and 2, respectively. On a given magnetic sublattice (site) there will, in general, be contributions from the (degenerate) spin up and spin down levels of the lower band and, also, from the spin up and spin down levels of the upper band. We write the respective probability of finding the spin 'up' or spin 'down' lower level as $0.5(1\pm\varepsilon_1)$ and the probability of finding an electron in the lower band as a_1.[1] Where necessary, to express differences in spin 'up' and spin 'down' radial matrix elements connecting the core and valence levels, a correction of the form, $(1\pm\delta_1)$, may be made to the mean radial matrix element, $M_{o,1}$, associated with transitions to the lower band. Analogous quantities are defined for the upper level, subscript 2. In general ε_2 is the negative of ε_1. In the following, the band splitting, $2g$, is assumed the same for all sub-bands of different orbital projection m_l and the spin–orbit splitting of the intermediate levels and the spin splitting of the core level are ignored.

In the limit that the band width, W, is much less than the inverse core hole lifetime, Γ, one may express the resonant amplitude as a sum over contributions from the lower band (subscript 1) and the upper band (subscript 2). Following [2]:

$$f \propto \frac{(1-a_1)(\alpha_1 M_1 - \beta_1 N_1)}{E_1} + \frac{(1-a_2)(\alpha_2 M_2 - \beta_2 N_2)}{E_2} \quad (1)$$

where, for $i = 1, 2$,

$$\alpha_i = 0.5(1+\varepsilon_i),\ M_i = M_{o,i}(1+\delta_i)$$

$$\beta_i = 0.5(1-\varepsilon_i),\ N_i = M_{o,i}(1-\delta_i)$$

and

$$E_{1,2} = \hbar\omega_i - E_o \pm g - i\Gamma$$

$E_o \pm g$ referring to $E_{1,2}$. E_o is the mean resonant scattering energy, and $\hbar\omega_i$ is the incident photon energy. The amplitude has the form of a lightly damped oscillator [2] where the damping, Γ in the denominator, arises from the finite width of the core level. The numerator is composed of three parts: $(1-a_i)$ gives the probability that the intermediate band i on the resonant ion is empty; α_i, β_i, express the relative weight of the intermediate state on the ion and M_i, N_i are the mean radial matrix elements for the transition (electric dipole, quadrupole, etc.) under consideration.

This gives the incident energy dependence of the cross-section as:

$$|f|^2 \propto \frac{A_1^2\left\{\Gamma^2 + \left(E_o - \hbar\omega_i + g\frac{A_2}{A_1}\right)^2\right\}}{\{(E_o - \hbar\omega_i - g)^2 + \Gamma^2\}\{(E_o - \hbar\omega_i + g)^2 + \Gamma^2\}} \quad (2)$$

where,

$$A_{1,2} = 0.5\left[M_{o,1}(1-a_1)(\varepsilon_1+\delta_1) \pm M_{o,2}(1-a_2)(\varepsilon_2+\delta_2)\right] \quad (3)$$

At a given absorption edge, i.e. given E_o and Γ, mindful that there is in principle a self-consistent coupling of a_i, ε_i, δ_i and g, this yields an empirical three parameter fit, A_1, A_2 and g, to the form of the resonant scattering cross-section.

For comparison, the single ion (ferromagnetic) case, where all m_l are equally occupied, is written as:

$$f \propto \frac{0.5(1-a\uparrow)(1+\delta)}{E_\uparrow} - \frac{0.5(1-a_\downarrow)(1-\delta)}{E_\downarrow} \quad (4)$$

where the 'up' and 'down' spin matrix elements have a values $M_o(1\pm\delta)$ respectively. The energy denominators are $E_{\uparrow,\downarrow} = E_o \pm \Delta - \hbar\omega_i - i\Gamma$ and the level occupations $a_{\uparrow,\downarrow}$. This gives the incident energy dependence of the cross-section as:

$$|f|^2 \propto \frac{\mathscr{A}_1^2\left\{\Gamma^2 + \left(E_o - \hbar\omega_i + \Delta\frac{\mathscr{A}_2}{\mathscr{A}_1}\right)^2\right\}}{\{(E_o - \hbar\omega_i - \Delta)^2 + \Gamma^2\}\{(E_o - \hbar\omega_i + \Delta)^2 + \Gamma^2\}} \quad (5)$$

where

[1] Since there is no exchange splitting, the probability of finding either a spin 'up' or a spin 'down' quasiparticle in a given band is the same. The Fermi functions are the same. The probability is taken independent of the orbital projection m_l, this ensures zero orbital angular momentum. Where necessary (e.g. in insulators) this constraint may be relaxed.

$$A_{1,2} = 0.5[M_o(1-a_\uparrow)(1+\delta) \mp M_o(1-a_\downarrow)(1-\delta)] \quad (6)$$

Once again, as in the antiferromagnetic case, the a, δ and Δ ought to be self-consistently determined. Empirically they are normally treated as independent variables.

To simplify the comparison between the single ion and antiferromagnetic forms we neglect δ, approximate $M_{o,1} = M_{o,2}$and set $\varepsilon_1 = -\varepsilon_2$. This yields for the antiferromagnet,

$$A_1 = 0.5M\varepsilon[a_2 - a_1]$$

$$A_2 = 0.5M\varepsilon[2 - a_2 - a_1],$$

and for the single ion,

$$\mathcal{A}_1 = 0.5M(a_\downarrow - a_\uparrow)$$

$$\mathcal{A}_2 = 0.5M(2 - a_\downarrow - a_\uparrow).$$

If the fractional occupancy (a_1, a_2) of the band is constant and the magnitude of ε, which measures the sublattice polarisation, is taken as an order parameter, c.f. $(a_\uparrow - a_\downarrow)$ in the atomic formulation, then A_1 indeed plays the role of an order parameter. However, in contrast with the single-ion result, A_2 is also proportional to the order parameter. Indeed it is rather the ratio A_1/A_2 that becomes a (temperature independent) measure of the electron count; for example, the case where the upper band is empty gives,

$$a_1 = \frac{2\left(\frac{A_1}{A_2}\right)}{\left(\frac{A_1}{A_2}\right) - 1}$$

enabling an estimate of the band filling. Thus the behavior of the empirical quantity A_1/A_2 in the vicinity of T_N may serve to distinguish the different model approaches. At this level neither model expresses the dynamical nor vector nature of the local magnetic moment. The former is dealt with in the following manner: Bragg-scattering measures that projection of the local moment which is the same on all sites within the photon coherence volume over the photon coherence time (quasi-static approximation). This time scale depends on the incident monochromaticity (typical values for high resolution X-ray~10^{-15}–10^{-14} s, c.f. neutron~10^{-10}–10^{-12} s). The vector nature of the quasi static projected moment enters the cross-section via a polarisation factor [1,2]. As noted, the quantities ε and $(a_\uparrow - a_\downarrow)$ are functionals of g and Δ respectively and, in general, since the latter collapse on heating to T_N, one anticipates that in either case the scattering cross-section will fall as the phase transition is reached.

2.2. Limiting forms of the antiferromagnetic cross-section

(i) First the case $A_1 = -A_2$,

$$|f|^2 \propto \frac{A_1^2}{\{(E_o - \hbar\omega_i + g)^2 + \Gamma^2\}}.$$

This arises when the lower band is full and one has a single level problem. This suggests that non-Lorentzian energy line shapes are more likely to occur below half filling. Practically, one would not often know the value of E_o to within the accuracy of g (typically on the scale of eV) and hence this would be seen as an ordinary resonance.

(ii) If the ratio g/Γ is small, or one is far from resonance, a two parameter fit (A_1, gA_2) may be possible,

$$|f|^2 \propto \frac{A_1^2}{\{(E_o - \hbar\omega_i)^2 + \Gamma^2\}}\left[1 + \frac{2(E_o - \hbar\omega_i)g\left(\frac{A_2}{A_1}\right)}{\{(E_o - \hbar\omega_i)^2 + \Gamma^2\}} + O(g^2)\right].$$

(iii) Total band occupation small (zero) together with the conditions, $M_{o,1} \approx M_{o,2}$, $\varepsilon_1 \approx -\varepsilon_2$ and δ negligible;

$$|f|^2 \propto \frac{g^2\varepsilon^2 M_o^2}{\{(E_o - \hbar\omega_i - g)^2 + \Gamma^2\}\{(E_o - \hbar\omega_i + g)^2 + \Gamma^2\}}.$$

As the antiferromagnetic band splitting, g, increases, the line shape acquires a flattened top, and eventually develops into a twin peaked structure when $g/\Gamma > 1$. [Similar effects are apparent in the general case on varying (A_2/A_1)]. This suggests that empty (d) bands, if polarised, for example by hybridisation, may have a non-Lorentzian in energy scattering profile. In this regime the scattering amplitude is dominated by the parameter A_2; $A_1 \to 0$. On increasing polarisation the parameter δ, signaling the difference between the spin 'up' and spin 'down' radial matrix elements may become significant, and indeed, at low temperatures as ε saturates, the behaviour of δ may be dominant [5].

2.3. Analysis of the Dy L_3 and L_2 magnetic resonant scattering in $DyFe_4Al_8$

Using the above formalism we overview an analysis made of the anomalous behaviour of the resonant magnetic scattering at the antiferromagnetic satellites in the compound $DyFe_4Al_8$ [4]. Neutron and X-ray experiments [6] show that the Fe sublattice orders magnetically at T_N~170 K with a small modification of the G-type AF structure [7]. Superimposed on the AF order is a cycloid modulation with q=[qq0], where q~0.14 reciprocal lattice unit at T_N. Below T_{Dy}~50 K there is a progressive (with reducing temperature) ordering of the long-range component of the Dy 4f moment [8]. The interest was to use the element specificity of the resonant cross-section to establish if a polarisation of the Dy 5d bands occurs, and, this being so, to follow its thermal evolution.

There are two remarkable features in the temperature dependence of the measured intensities at the $L_{2,3}$ edges. First is that the intensity of the resonance, integrated over energy and scattering angle, at the Dy L_3 edge *falls* as the sample is heated to T_N whilst that at the L_2 edge initially

rises, for 12 K$<T<T_{Dy}$, and then also falls to T_N as shown in Fig. 1. This effect naturally generates a temperature-dependent branching ratio (the ratio of the intensities at the L_3 to L_2 edges). The second point is that these intensity changes are accompanied by significant shifts in line shape and centre of mass of the resonance, Fig. 2. Polarisation analysis shows all spectra to have essentially pure electric dipole character, indeed, extensive modeling assuming the presence of either a strong non-resonant signal or a strong quadrupole signal or a combination of both taken together with an electric dipole peak has been unable to reproduce the temperature-dependent line shapes.

For $T_{Dy}<T<T_N$ the magnetic polarisation at the Dy site is weak [6,8], in this temperature range we set $\delta_1=\delta_2=0$. The ratio A_1/A_2 then yields an estimate of 2.2 electrons for the occupancy of the lower band (averaged over the L_2, L_3 edges with the upper band taken to be empty). This is in agreement with estimates based on band-structure calculations which give approximately two electrons [9]. We plot the ratio of the sum and difference of the parameters, A_2 and A_1, normalised to an occupancy of two electrons (the factor of 1.25 on the ordinate scale), in the insert to Fig. 1. As anticipated within the antiferromagnetic model, from T_N down to T_{Dy} the quantity is close to unity, however below this latter temperature, important deviations are seen. It is suggested that these may arise due to an increase of δ_1, δ_2 occasioned by the increasing ordered component of the Dy 4f moment. This 4f moment has been observed in neutron diffraction, and, indirectly via a concomitant lattice distortion, observed in non-resonant charge scattering at the $2q$ satellites. The temperature dependence of the latter, indicated by the filled diamond symbols in the insert to Fig. 1, is seen to closely follow the deviation of the normalised sum and difference of A_2 and A_1.

3. Discussion

3.1. Extension to bands of finite width

In this section we extend the method to intermediate resonant levels having a density of (vacant) states bandwidth important on the scale of Γ. We consider transitions via intermediate states characterised by an appropriate density of states $D(E)$ where $D(E)$ is an effective (projected) density of states of the correct symmetry. For example, the $2p\rightarrow 5d\rightarrow 2p$ transition considered in $DyFe_4Al_8$ re-

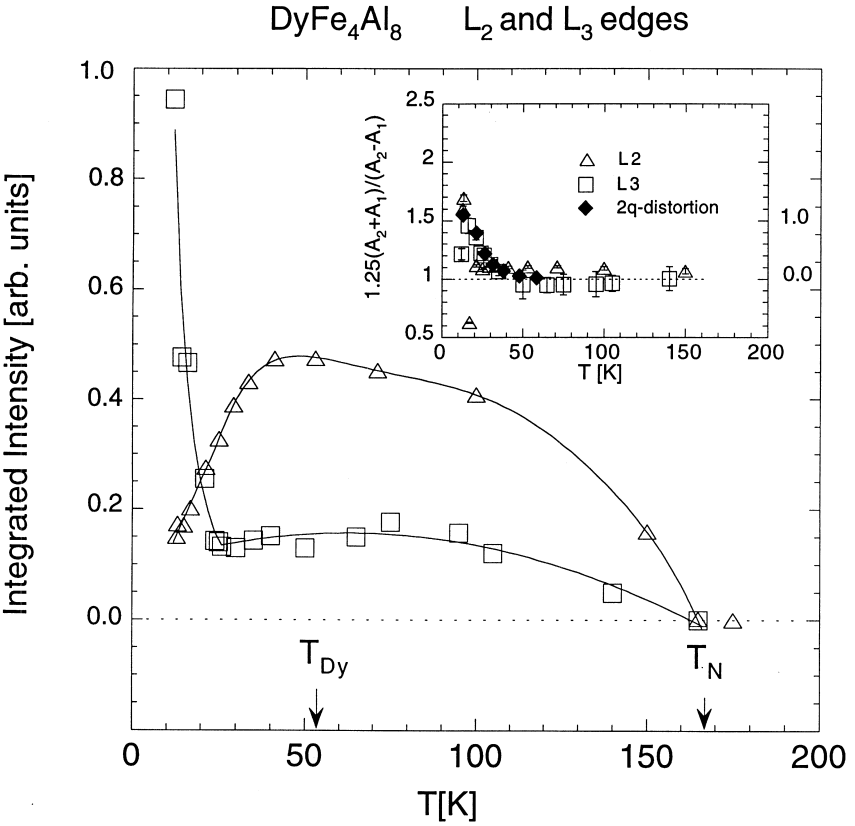

Fig. 1. Temperature dependence of the energy integrated intensity of the $(440)+q$ satellite in the $\sigma\rightarrow\pi$ channel as measured at the L_2 (open triangles) and L_3 (open squares) edges of dysprosium. These intensities have not been corrected for the small difference in absorption at the two edges. The lines through the points are a result of calculations using the narrow-band model presented in Section 2.1. The insert gives the temperature evolution of the ratio of parameters A_1 and A_2 from the fits normalised to a 5d band occupation of two electrons. The filled diamonds (right hand ordinate) show the temperature dependence of the $2q$ charge satellite (non-resonant $\sigma\rightarrow\sigma$ channel).

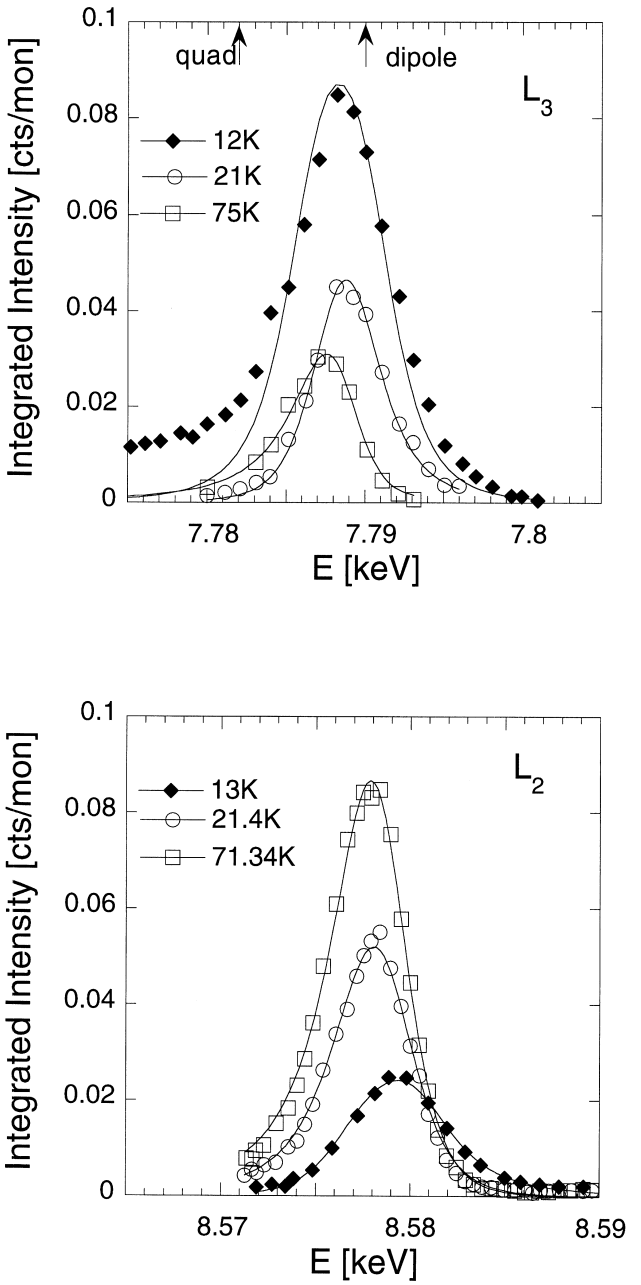

Fig. 2. Incident photon energy dependence of the angle-integrated scattering at the Dy L_3 (upper panel) and L_2 (lower panel) edges as measured at different temperatures at the (440)+q satellite in the $\sigma \rightarrow \pi$ channel. The solid lines result from the narrow-band approximation described in Section 2.1. There is one overall scale factor for the upper and lower figures, and, at a given temperature the fitted parameters, A_1, A_2 and g, have, within the experimental error, the same values at both edges.

quires the d or $l=2$ projection. At a given incident photon energy, ω_i, one is sensitive to the resonant contributions integrated over the bandwidth W. Assuming the matrix elements may be represented by some mean, energy independent, value over W:

$$f \propto \int_{E_1}^{E_1+W_1} \mathrm{d}E \, \frac{B_1 D_1(E)}{\hbar\omega_i - E - i\Gamma} + \int_{E_2}^{E_2+W_2} \mathrm{d}E \, \frac{B_2 D_2(E)}{\hbar\omega_i - E - i\Gamma} \quad (7)$$

here E_1 is the bottom of the lower energy band which is split by the antiferromagnetic potential by an amount $2g$ from the lower edge of the upper band at E_2. $B_1 = (A_1 + A_2)/2$ and $B_2 = (A_1 - A_2)/2$ where $A_{1,2}$ are defined in Eq. (3). Consider the structure of the integral,

$$\int_{E}^{E+W} \mathrm{d}E \, \frac{D(E)}{\hbar\omega_i - E - i\Gamma} = \int_{E}^{E+W} \mathrm{d}E \, D(E) \left[G_{\mathrm{Re}}(\hbar\omega_i - E, \Gamma) + iG_{\mathrm{Im}}(\hbar\omega_i - E, \Gamma) \right] \quad (8)$$

that is, the scattering amplitude is proportional to a modified density of states given by the convolution, $\bar{D}(\hbar\omega_i)$, of $D(E)$ with G_{Re} and G_{Im} where

$$G_{\mathrm{Re}}(\hbar\omega_i - E, \Gamma) = \frac{\hbar\omega_i - E}{(\hbar\omega_i - E)^2 + \Gamma^2}$$

and

$$G_{\mathrm{Im}}(\hbar\omega_i - E, \Gamma) = \frac{\Gamma}{(\hbar\omega_i - E)^2 + \Gamma^2}$$

This gives:

$$f \propto B_1 \bar{D}_{\mathrm{lower}}(\hbar\omega_i) + B_2 \bar{D}_{\mathrm{upper}}(\hbar\omega_i) \quad (9)$$

In general the diffraction energy profile is dominated by the width of $D(E)$ which can be much larger than either g or the inverse core hole lifetime, Γ. Given both B_1 and B_2 are proportional to the band polarisation, ε, the intensity will depend on the square of the antiferromagnetic polarisation.

Once the density of states has been smoothed over the inverse core hole lifetime, for small band splitting, g, on the scale of Γ, one may write:

$$f \propto [B_1 + B_2]\bar{D}_{E_o} + g[B_1 - B_2] \frac{\mathrm{d}\bar{D}_{E_o}}{\mathrm{d}\hbar\omega_i} \quad (10a)$$

or

$$f \propto A_1 \bar{D}_{E_o} + gA_2 \frac{\mathrm{d}\bar{D}_{E_o}}{\mathrm{d}\hbar\omega_i} \quad (10b)$$

giving

$$f \propto \varepsilon M(a_2 - a_1)\bar{D}_{E_o} + g\varepsilon M(2 - a_1 - a_2) \frac{\mathrm{d}\bar{D}_{E_o}}{\mathrm{d}\hbar\omega_i} \quad (10c)$$

where on neglecting the matrix element corrections in Eq. (10c), we have set $B_1 = \varepsilon M(1 - a_1)$ and $B_2 = -\varepsilon M(1 - a_2)$. These limiting forms also serve to illustrate the general shape of the cross-section without explicit numerical analysis. In the narrow-band limit $D(E)$ is approximated as a Dirac delta function and one recovers the results of Section (2.2.ii). When the bandwidth is (much)

greater than Γ, the real part of $\bar{D}(\hbar\omega_i)$, given by integration of $D(E)$, positive definite, over G_{Re} which is odd in its argument, may make a small contribution with respect to the integration over the imaginary part, G_{Im}, which is an even function. Consequently, as a first approximation, one may neglect the real part. This reduces the scattering amplitude for wide bands to the sum of the Lorentzian smeared density of (vacant) states and its derivative.

In Eq. (10a), the sum, $B_1 + B_2$, which varies with the difference in occupation of the antiferromagnetically split bands, will be small when both bands are empty. In contrast, the coefficient of the derivative remains finite until both bands are full giving, in parallel with the narrow band considerations, a multi-peaked structure to transitions involving polarised empty bands. The modified density of states, $D(\hbar\omega_i)$, will rise and fall as one passes from the bottom to the top of an unoccupied band. At the rising edge the derivative is positive, at the maximum (maxima) it vanishes, and on the falling edge it is negative. Thus the energy dependent profile may become lopsided and, even for a symmetric $D(E)$, may exhibit more than one maximum depending on the band occupation.

In the derivation, a core level with spin–orbit splitting much greater than Γ has been assumed [2] whilst the spin–orbit splitting of the intermediate states has been ignored. When spin–orbit coupling, ζ_{so}, of the intermediate states becomes important, as for example at the K and L_1 edges, one anticipates a term of the order,

$$f \propto \zeta_{\mathrm{so}}\, g\, \frac{\mathrm{d}^2 \bar{D}_{E_o}}{\mathrm{d}\hbar\omega_i^2} \tag{12}$$

Eq. (12) will give, from a smooth $\bar{D}_{E_o}$, an even more structured energy profile. For example, from a Lorentzian profile one obtains a sharp central peak flanked, on either side, by a minor peak of ~8% intensity. It will be of interest to look for such line shapes to help establish the range of the formalism.

We proceed to give two examples. The first is the case of the rectangular $D(E)$ evaluated using Eq. (7). The second, an application of Eq. (10) to estimate the width of the resonant energy profile using a calculated $D(E)$ for the Dy 5d bands in the compound $DyFe_4Al_8$.

3.2. Rectangular D(E)

In the case where $D(E)$ may be represented by a rectangular form, the integrals in Eq. (7) give,

$$f \propto B_1\left[\frac{1}{2}\ln\left[\frac{(\hbar\omega_i - E_1)^2 + \Gamma^2}{(\hbar\omega_i - E_1 - W_1)^2 + \Gamma^2}\right] + i\left\{\tan^{-1}\left(\frac{\hbar\omega_i - E_1}{\Gamma}\right) - \tan^{-1}\left(\frac{\hbar\omega_i - E_1 - W_1}{\Gamma}\right)\right\}\right] + B_2\left[\frac{1}{2}\ln\left[\frac{(\hbar\omega_i - E_2)^2 + \Gamma^2}{(\hbar\omega_i - E_2 - W_2)^2 + \Gamma^2}\right] + i\left\{\tan^{-1}\left(\frac{\hbar\omega_i - E_2}{\Gamma}\right) - \tan^{-1}\left(\frac{\hbar\omega_i - E_2 - W_2}{\Gamma}\right)\right\}\right] \tag{13}$$

The regimes of parameters give different characteristically shaped energy profiles. As noted above, the symmetry ensures that when the photon energy is at the midpoint of W, the amplitude has no contribution from the real (logarithmic) term, and this will lead, depending on the relative parametric values to a flattening of the resonant response profile and eventually to the formation of two peaks. Some example profiles are given in Fig. 3. A given density of electronic states may be modeled as a sum of rectangles (histogram) and the above formula generalised in an obvious way.

3.3. A model calculation

The *D(E)* for the Dy 5d bands in the compound $DyFe_4Al_8$ has been calculated for a ferromagnetic polarisation [9]. For an illustration of the use of the above formalism we use the down-spin density of empty states as representative of $D_o(E)$, the up-spin density has a similar energy profile. For the characteristic energy of the Dy L_3 edge and the core hole life time (Γ~1.7 eV) we appeal to the literature [10]. In Fig. 4, left panel, we give the calculated $D(E)$ and the real and imaginary parts of $\bar{D}(\hbar\omega_i)$. Fig. 4, right panel, gives the cross-section in comparison with the measured scattering as a function of the incident photon energy calculated using the first term in Eq. (10). The agreement of line shape is reasonable considering there are no adjustable parameters apart from the overall amplitude. It appears then, that the width of the observed resonance (Γ~4 eV) may fail to be a good indicator of the core hole line width at the Dy L edges. It should be recalled that the starting $D(E)$ had no antiferromagnetic splitting and the calculation does not include the derivative term (g set to zero). Qualitatively, narrowing the bandwidth by including the antiferromagnetic splitting and the addition of the derivative term will both tend to give a more peaked cross-section in accordance with experiment.

3.4. Fluorescence

The fluorescence at an absorption edge may be modeled in terms of a density of states [11–13]. This density of states is to be chosen to mimic the dynamical (many body) effect of the transient core hole; numerical studies suggest one may use the density of final states [11,13]. Empirically, one may analyse the intensity in a similar manner to the scattering considered above but with coefficients $B_1 = M(1 - a_1)$ and $B_2 = M(1 - a_2)$ where we assume the same fluorescence yield for both bands. This gives, for $g < \Gamma$:

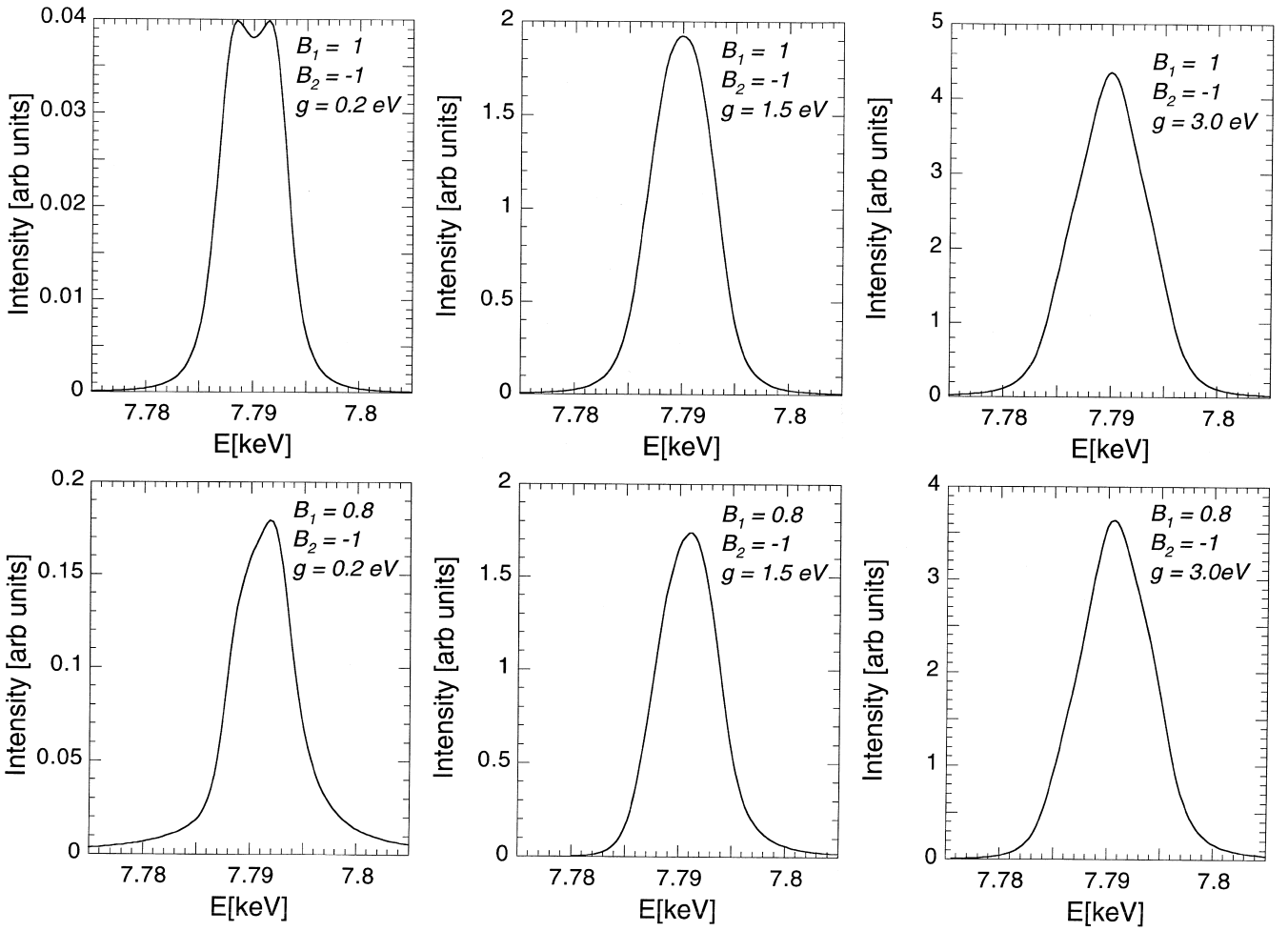

Fig. 3. Examples of energy profiles coming from rectangular density of states. From left to right the upper three panels give the computed profiles for a band width of 5 eV; $\Gamma = 2$ eV; $B_1 = 1 = -B_2$ and $g = 0.2$, 1.5, 3 eV. This roughly models empty bands. Below, also from left to right, with the similar parameters except $B_1 = 0.8$ and $B_2 = -1$.

$$f'' \propto \mathrm{Im}\,\bar{D}_{E_o} M[2 - (a_2 + a_1)] + g\frac{\mathrm{d}\,\mathrm{Im}\,\bar{D}_{E_o}}{\mathrm{d}\hbar\omega_i} M(a_2 - a_1) \tag{11}$$

where Im $\bar{D}(\hbar\omega_i)$ is the imaginary part of $\bar{D}(\hbar\omega_i)$ given in Eq. (7) above. The profile is dominated by the core hole smeared density of states. In the approximation that the fluorescence is an incoherent process, it appears appropriate to use a local density of states (summed over all wave vectors) projected on the final states [12]. For the coherent scattering considered in the previous section, such an approximation may be less certain; first the scattering involves absorption followed by emission, second, the coherence implies a wave vector selection. At the empirical level, the low energy tail of the fluorescence spectra is dominated by, and hence may be used to estimate, the core hole lifetime. Given the core hole lifetime, the profile may be used to estimate the density of available states, which, if the absorption and scattering are both electric dipole dominated, will be of the appropriate symmetry. The problem is more delicate for the electric quadrupole terms where the imaginary part may be relatively weak. At a first level of approximation this gives an empirical basis on which to model the dipole-induced antiferromagnetic scattering cross-section [14].

4. Conclusion

An elementary model of resonant X-ray diffraction in antiferromagnetic materials has been presented in two stages. In the narrow-band limit $W \ll \Gamma$, the band width, W, drops out of the problem. This is the simplest scenario in which to introduce the concept of spatial magnetic order with degeneracy in energy as opposed to an atomic model where the energy splitting of up and down spin orbitals is used to generate a magnetic cross-section. We have shown that, formally, the narrow-band antiferromagnetic and the atomic expressions for the cross-section may be arranged to look rather similar, indeed at the level where one neglects the band splitting (g), or equivalently the exchange splitting (Δ), they appear essentially identical.

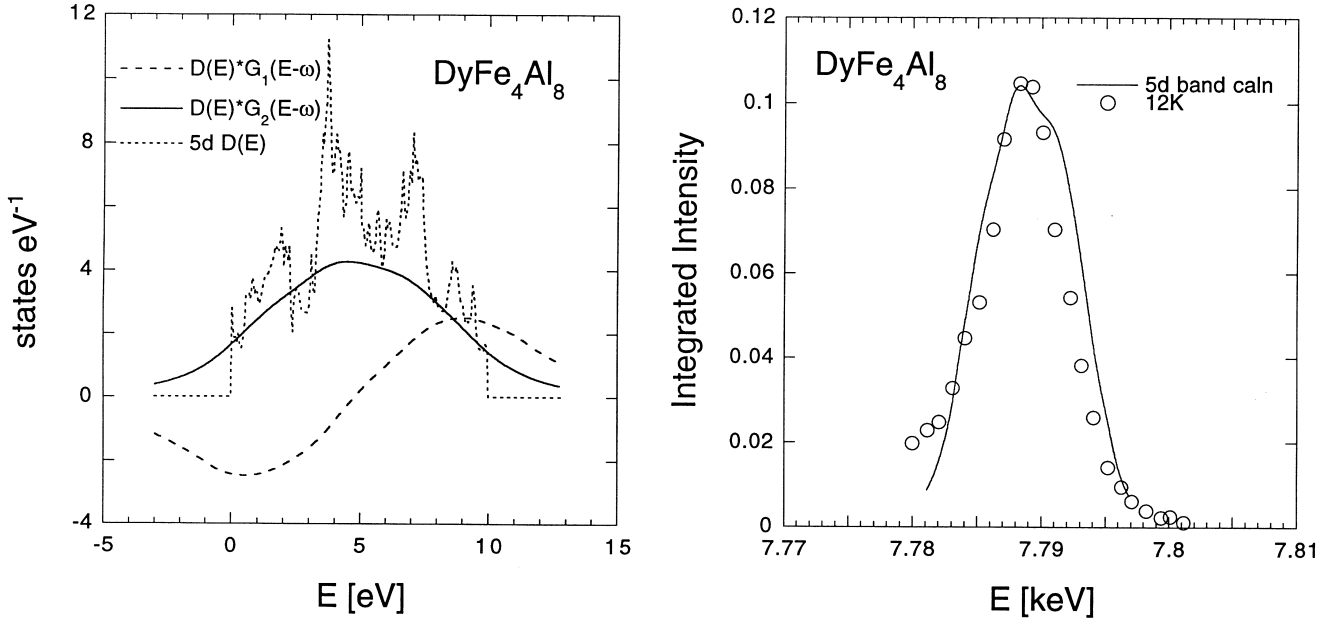

Fig. 4. Left panel gives 5d projected D(E) for $DyFe_4Al_8$ [9] and the real and imaginary contributions to $\bar{D}_{E_0}$. Right panel gives the calculated intensity of the L-edge resonance, here compared with the L_3 data at 12 K.

However, as stressed, they do have important differences in interpretation.

The influence of a wide distribution of intermediate states has then been considered. It is noted that, in addition to cases where absorption plays a dominant role [15], diffraction energy profiles with non-Lorentzian line shapes (e.g. flatten tops, faster then Lorentzian tails, multiple peaked structures), or excessive line widths as compared with the anticipated core hole life time may find a simple interpretation. For example, the L-edge scattering from the rare earth metals Dy and Lu have been reported with a half width $\Gamma = 3.5$ eV [16], the anticipated value for the inverse core hole lifetime is ~1.7 eV [10]. In a similar vein, the analysis of the complex behaviour of the $DyFe_4Al_8$ $L_{2,3}$ profiles given in Ref. [4] in the narrow-band limit uses an effective inverse core hole lifetime corresponding with $\Gamma = 3.5$ eV. Our calculations in Section 3.3 show that the origin of this effective core hole lifetime may lie in the energy bandwidth of the 5d intermediate states, $D(E)$. More complete analysis of L-edge rare earth and actinide spectra, based on the effective (projected) $D(E)$ calculated in the antiferromagnetic state, are clearly desirable.

Acknowledgements

This work was stimulated by experiments carried out on the ID20 beamline at European Synchrotron Radiation Facility, Grenoble. I thank my colleagues for their advice and critique which has contributed to this work. The ITU Karlsruhe and ILL Grenoble are thanked for their support during the course of this work.

References

[1] G. Materlik, C.J. Sparks, K. Fisher (Eds.), Resonant Anomalous X-ray Scattering, Theory and Applications, Elsevier Science B.V, 1994.
[2] J.P. Hannon, G.T. Trammell, M. Blume, D. Gibbs, Phys. Rev. Lett. 61 (1988) 1245.
[3] E. Arola, P. Strange, B. Gyorffy, Phys. Rev. B55 (1997) 472.
[4] S. Langridge et al., Phys. Rev. Lett. 82 (1999) 2187.
[5] M. van Veenendaal et al., Phys. Rev. Lett. 78 (1997) 1162.
[6] J.A. Paixão et al., to be published.
[7] P.C.M. Gubbens et al., J. Magn. Magn. Mater. 27 (1982) 61.
[8] W. Schäffer, G. Will, J. Less Common Metals 94 (1983) 205.
[9] M. Brooks, private communication.
[10] W. Bambynek, B. Crasemann et al., Rev. Mod. Phys. 44 (1972) 716.
[11] J.E. Muller, O. Jepsen, O.K. Andersen, J.W. Wilkins, Phys. Rev. Lett. 40 (1978) 720.
[12] U. von Barth, G. Grossmann, Solid State Comm. 32 (1979) 645.
[13] P. Nozieres, C.T. DeDominicis, Phys. Rev. 178 (1969) 1097.
[14] A. Stunault et al. Phys. Rev. B (1999) submitted.
[15] N. Bernhoeft et al., Phys. Rev. Lett. 81 (1998) 3419.
[16] B.A. Everitt et al., Phys. Rev. Lett. 75 (1995) 3182.